ELSEVIER

Biochemical Pharmacology 64 (2002) 1533–1546

Biochemical Pharmacology

Cellular energetics and glutathione status in NRK-52E cells: toxicological implications

Lawrence H. Lash*, David A. Putt, Sarah E. Hueni, Wei Cao, Feng Xu, Stephen J. Kulidjian, Judith P. Horwitz

Department of Pharmacology, Wayne State University School of Medicine, 540 East Canfield Avenue, Detroit, MI 48201, USA

Received 18 September 2001; accepted 17 April 2002

Abstract

Cellular energetics and redox status were evaluated in NRK-52E cells, a stable cell line derived from rat proximal tubules. To assess toxicological implications of these properties, susceptibility to apoptosis induced by *S*-(1,2-dichlorovinyl)-L-cysteine (DCVC), a well-known mitochondrial and renal cytotoxicant, was studied. Cells exhibited high activities of several glutathione (GSH)-dependent enzymes, including γ-glutamylcysteine synthetase, GSH peroxidase, glutathione disulfide reductase, and GSH *S*-transferase, but very low activities of γ-glutamyltransferase and alkaline phosphatase, consistent with a low content of brush-border microvilli. Uptake and total cellular accumulation of [^{14}C]α-methylglucose was significantly higher when cells were exposed at the basolateral as compared to the brush-border membrane. Similarly, uptake of GSH was nearly 2-fold higher across the basolateral than the brush-border membrane. High activities of ($Na^+ + K^+$)-ATPase and malic dehydrogenase, but low activities of other mitochondrial enzymes, respiration, and transport of GSH and dicarboxylates into mitochondria were observed. Examination of mitochondrial density by confocal microscopy, using a fluorescent marker (MitoTracker® Orange), indicated that NRK-52E cells contain a much lower content of mitochondria than rat renal proximal tubules *in vivo*. Incubation of cells with DCVC caused time- and concentration-dependent ATP depletion that was largely dependent on transport and bioactivation, as observed in the rat, on induction of apoptosis, and on morphological damage. Comparison with primary cultures of rat and human proximal tubular cells suggests that the NRK-52E cells are modestly less sensitive to DCVC. In most respects, however, NRK-52E cells exhibited functions similar to those of the rat renal proximal tubule *in vivo*.

Keywords: Cellular energetics; Glutathione; Kidney; NRK-52E cells; *S*-(1,2-Dichlorovinyl)-L-cysteine; Apoptosis

1. Introduction

Renal PT cells have large requirements for metabolic energy and for the maintenance of redox status because of the high activities of active transport processes and other energy-requiring, biosynthetic reactions. These cells also possess a unique combination of mechanisms for the handling of GSH, a principal cellular antioxidant and cosubstrate in numerous drug metabolism reactions. These mechanisms include carrier-mediated transport across the brush-border and basolateral plasma membranes and mitochondrial inner membrane, extracellular degradation by the BBM enzyme GGT, intracellular synthesis of GSH from precursor amino acids, and a full complement of GSH-dependent enzymes involved in drug metabolism and detoxification of reactive electrophiles and oxidants [1,2].

To study the function and molecular biology of proteins of renal PT origin from the rat, a cell line derived from the rat proximal tubule is needed. NRK-52E cells are the natural choice for these studies because they are derived from **n**ormal **r**at **k**idney proximal tubules. Unfortunately,

* Corresponding author. Tel.: +1-313-577-0475; fax: +1-313-577-6739.
E-mail address: l.h.lash@wayne.edu (L.H. Lash).

Abbreviations: AMG, α-methylglucose; AOAA, aminooxyacetic acid; AP, alkaline phosphatase; BBM, brush-border membrane; BLM, basolateral membrane; DCVC, *S*-(1,2-dichlorovinyl)-L-cysteine; DMEM, Dulbecco's Modified Eagle's Medium; FACS, fluorescence-activated cell sorter; F344, Fischer-344; GCS, γ-glutamylcysteine synthetase; GDH, glutamate dehydrogenase; GGT, γ-glutamyltransferase; GPX, glutathione peroxidase; GRD, glutathione disulfide reductase; GSH, glutathione; GSSG, glutathione disulfide; GST, GSH *S*-transferase; IAA, iodoacetate; LDH, lactate dehydrogenase; MDH, malic dehydrogenase; PAH, *p*-aminohippurate; PT, proximal tubular; SD, Sprague–Dawley; SDH, succinate dehydrogenase; STS, staurosporine.

0006-2952/02/$ – see front matter
PII: S0006-2952(02)01360-6

the biochemical function of these cells has not been characterized extensively, particularly with respect to mitochondrial function or GSH status. Woods and colleagues [3] used NRK-52E cells to study the up-regulation of GSH biosynthesis as an adaptation to chronic oxidative stress. These studies demonstrated the capability of the cell line to respond to conditioning with chronic exposure to an oxidant (by treatment with diethylmaleate) by increasing the production of GCS mRNA and protein. Miller *et al.* [4] used NRK-52E cells to study oxalate-induced apoptosis and necrosis. Their studies showed that oxalate causes both forms of cell death, thus demonstrating the utility of this cell culture model for studying such processes.

The goals of the present study were to determine activities of several key enzymes involved in cellular energetics and GSH metabolism, to compare these with those in rat renal proximal tubules, and to characterize the transport, metabolism, and subcellular distribution of transported GSH. Finally, the cytotoxicity of a renal PT toxicant that is known to target mitochondria was characterized to test the hypothesis that these cells respond similarly as the *in vivo* proximal tubule and that they are a suitable model for future studies on GSH transport and mitochondrial function.

2. Materials and methods

2.1. Chemicals and materials

STS, double-processed, tissue culture water, PAH, AOAA, and digitonin (aqueous type, recrystallized twice from hot ethanol before use) were purchased from the Sigma Chemical Co. Silicone oil (high temperature, $n_D = 1.4950$ at 20°, $d = 1.050$) and mineral oil (white, light paraffin oil, $n_D = 1.4760$ at 20°, $d = 0.862$) were purchased from the Aldrich Chemical Co. Vitrogen (purified collagen in 0.012 N HCl) was purchased from Cohesion Technologies. Cell culture medium [DMEM containing 4 mM L-glutamine, 1.5 g/L of $NaHCO_3$, 4.5 g/L of glucose, 1 mM sodium pyruvate, and 5% (v/v) calf serum] was purchased from the American Type Culture Collection (Catalogue No. 30-2002). MitoTracker® Orange CMTRos was purchased from Molecular Probes. DCVC was synthesized from trichloroethylene and L-cysteine as described previously [5]. Purity (>95%) was determined by HPLC analysis, and identity was confirmed by proton nuclear magnetic resonance spectroscopy. Impurities were likely degradation products of trichloroethylene and L-cysteine and are unlikely to contribute significantly to any observed, cytotoxic response. As it is very laborious and impractical to try and improve the purity of the DCVC, no additional purification was attempted. 3-*O*-[^{14}C]AMG (specific activity 53 mCi/mmol) and [^{3}H-*glycyl*]GSH (44.8 Ci/mmol) were purchased from NEN Dupont. All other chemicals were of the highest purity available and were obtained from commercial sources. NRK-52E cells were purchased from the American Type Culture Collection (Catalogue No. CRL-1571). Polystyrene tissue culture flasks (T-25, T-75) or 35-mm culture dishes were from either Corning or Falcon-Becton Dickinson. Millicell polycarbonate filter inserts (0.4 μm pore size, 30 mm diameter) were purchased from Millipore.

2.2. Cell culture procedures

NRK-52E cells (0.4×10^4/cm^2; 0.5×10^6/mL) were cultured on either collagen-coated polystyrene culture flasks (T-25 [3 mL total volume] or T-75 [11 mL total volume]), collagen-coated 35-mm polystyrene culture dishes (1 mL total volume), or collagen-coated polycarbonate filter inserts in 35-mm polystyrene culture dishes (1 mL total volume in the upper compartment, 0.5 mL total volume in the lower compartment) with DMEM supplemented as described above in an atmosphere of 5% CO_2/95% air at 37°. The choice of culture surface depended on the specific needs of each experiment, and is detailed below. Upon reaching confluence (5–9 days), subcultures were prepared by a 15-min treatment with 0.02% (w/v) EDTA, 0.05% (w/v) trypsin solution and replating the cells at a density of 4×10^4/cm^2. All enzyme, ATP, transport, and metabolism assays, and all flow cytometry and confocal microscopy experiments were performed with cell cultures that had just reached confluence.

2.3. Enzyme assays and protein determination

2.3.1. Cellular energetics enzymes

AP (EC 3.1.3.1) activity was measured with *p*-nitrophenylphosphate as substrate by the absorbance change at 410 nm, using $\varepsilon = 17{,}000\ M^{-1}\ cm^{-1}$ [6]. ($Na^+ + K^+$)-stimulated ATPase (EC 3.6.1.3) activity was measured as the vanadate-inhibitable activity coupled to NADH oxidation, and was determined as the absorbance change at 340 nm, using $\varepsilon = 6220\ M^{-1}\ cm^{-1}$ [7]. SDH (EC 1.3.99.1) activity was measured by coupling succinate oxidation to ferricytochrome *c* reduction and measuring the increase in absorbance at 550.5 nm, using $\varepsilon = 18{,}500\ M^{-1}\ cm^{-1}$ [8]. Activities of GDH (EC 1.4.1.2), LDH (EC 1.1.1.27), and MDH (EC 1.1.1.37) were measured as NADH oxidation by coupling to 2-oxoglutarate, pyruvate, and malate reduction, respectively, and determining the absorbance change at 340 nm, using $\varepsilon = 6220\ M^{-1}\ cm^{-1}$ [9–11].

2.3.2. GSH-dependent enzymes

GCS (EC 6.3.2.2) activity was measured with L-α-aminobutyrate as an L-cysteine analogue and coupling to NADH oxidation at 340 nm, using $\varepsilon = 6220\ M^{-1}\ cm^{-1}$ [12]. GPX (EC 1.11.1.9) activity was measured with 0.25 mM H_2O_2 as substrate and was equated to NADPH oxidation as detected by the decrease in absorbance at 340 nm, using $\varepsilon = 6220\ M^{-1}\ cm^{-1}$ [13]. GRD (EC

1.6.4.2) activity was measured as NADPH oxidation by the decrease in absorbance at 340 nm, using $\varepsilon = 6220\ M^{-1}\ cm^{-1}$ [14]. GGT (EC 2.3.2.2) activity was measured with γ-glutamyl-*p*-nitroanilide and glycylglycine as substrates and detection of *p*-nitroanilide formation at 410 nm, using $\varepsilon = 8800\ M^{-1}\ cm^{-1}$ [15]. GST (EC 2.5.1.18) activity was measured with 1-chloro-2,4-dinitrobenzene as substrate and detection of *S*-2,4-dinitrophenyl GSH formation at 340 nm, using $\varepsilon = 9600\ M^{-1}\ cm^{-1}$ [16].

Protein concentration of cells was measured with the bicinchoninic acid protein determination kit from Sigma, using bovine serum albumin (0.1–0.6 mg/mL) as a standard.

2.4. Confocal microscopy

Mitochondria in NRK-52E cells were localized by using a mitochondrial fluorescent marker (MitoTracker® Orange CMTRos), which is orange/red and has excitation and emission wavelengths of 552 and 576 nm, respectively. NRK-52E cells were grown on collagen-coated, glass coverslips in 35-mm dishes and were viewed with a Zeiss Triple-Laser Scanning Confocal Microscope (LSM 30) with an integrated work station at the Confocal Imaging Core Facility in the School of Medicine at Wayne State University. This is a core facility of the NIEHS Center for Molecular Toxicology with Human Applications at Wayne State. To obtain photomicrographs of cells treated with medium (=Control), DCVC, or STS, cells were grown on collagen-coated, 35-mm culture dishes and were viewed with the Zeiss Triple-Laser Scanning Confocal Microscope (LSM 30). Initial magnification in both cases was 196×.

2.5. Measurement of AMG and GSH transport

NRK-52E cells were grown on collagen-coated, Millicell-PCF inserts in 35-mm culture dishes, and were incubated with either 1 mM 3-*O*-[^{14}C]AMG or 5 mM [^{3}H-*glycyl*]GSH added to either the lower (=basolateral) or upper (=brush border) compartment at 37° for 0.5, 1, 2, 3, 5, 10, 15, or 30 min. At the end of the incubations, media were removed and cells were washed twice with PBS and were solubilized in 0.25 mL of 1% (w/v) SDS. Total cellular AMG or GSH uptake was quantitated by determination of radioactivity using a scintillation counter. Potential complications for accurate transport measurements due to intracellular metabolism of transported substrate was not a concern because AMG is a non-metabolizable analogue of D-glucose. Similarly, as detailed below, minimal metabolism of GSH occurs in these cells, especially during the relatively short time course of these transport measurements, allowing us to equate intracellular radioactivity with GSH content. The coincidence of ^{3}H-label with GSH on an HPLC chromatogram verified that no significant breakdown of radiolabeled GSH occurred during the transport experiments (data not shown).

2.6. Measurement of GSH and related metabolites by HPLC

Cellular contents of GSH, GSSG, L-glutamate, L-cysteine, and L-cystine were determined by ion-exchange HPLC on a Waters μBondapak amine cartridge (8 mm × 10 cm) (Waters Associates) after derivatization of thiols with iodoacetate and amine groups with 1-fluoro-2,4-dinitrobenzene [17,18]. Derivatives were detected by absorbance at 365 nm and were compared to authentic standards (limit of detection = 50 pmol).

2.7. Measurement of adenine nucleotides by HPLC

Intracellular contents of adenine nucleotides were measured in neutralized perchloric acid extracts by the HPLC method of Jones [19], as described previously [20]. Separation of ATP, ADP, and AMP was achieved by reversed-phase HPLC with a Waters μBondapak C_{18} cartridge (8 mm × 10 cm) (Waters Associates), and detection was by absorbance at 260 nm.

2.8. Digitonin fractionation and analysis of mitochondrial GSH content

Analysis of subcellular distribution of endogenous and transported GSH in NRK-52E cells was performed by detaching cells from culture dishes with brief trypsin-EDTA treatment and separation of cytoplasmic and mitochondrial compartments by digitonin fractionation [21]. Briefly, microcentrifuge tubes (1.5-mL capacity) were prepared in advance with three layers (from the bottom): 0.25 mL of 40% (v/v) glycerol, 0.5 mL silicone:mineral oil mixture (6:1), and 0.1 mL of 2-(*N*-morpholino)ethane sulfonic acid (MES) buffer (19.8 mM EDTA, 19.8 mM EGTA, 250 mM D-mannitol, 19.8 mM MES, pH 7.4) ± 0.15 mg of digitonin. An aliquot of suspended NRK-52E cells (0.5 mL, 10^{6} cells/mL) was mixed rapidly with the top layer, and the tubes were centrifuged at 13,000 *g* for 3 min at 22°. GSH content was measured in acid extracts of supernatants and resuspended glycerol-layer pellets by ion-exchange HPLC after derivatization with IAA and 1-fluoro-2,4-dinitrobenzene, as described above.

2.9. Flow cytometric analysis of the cell cycle

Cell cultures were washed twice with sample buffer (PBS plus 1 g glucose/L filtered through a 0.22-μm filter), dislodged by trypsin/EDTA incubation, centrifuged at 400 *g* for 10 min at 22°, and resuspended in sample buffer. Cell concentrations were adjusted to 1–3 × 10^{6}/mL with sample buffer, and 1 mL of the cell suspension was centrifuged at 400 *g* for 10 min at 22°. All of the supernatant except 0.1 mL/10^{6} cells was removed, and the remaining cells were mixed on a vortex mixer in the remaining fluid

for 10 sec. Next, 1 mL of ice-cold ethanol (70%, v/v) was added to the sample drop by drop, with samples being mixed for 10 sec between drops. The tubes were capped and fixed in ethanol at 4°. After fixing, the cells were stained in propidium iodide (50 μg/mL) containing RNase A (100 U/mL). Samples were then mixed, centrifuged at 1000 *g* for 5 min at 22°, and all the ethanol except for 0.1 mL was removed. Cells were mixed in the residual ethanol, and 1 mL of the propidium iodide staining solution was added to each tube. After mixing again, cells were incubated at room temperature for at least 30 min. Samples were analyzed within 24 hr by flow cytometry using a Becton Dickinson FACS*Calibur* Flow Cytometer, which is a core facility of the NIEHS Center for Molecular Toxicology with Human Applications at Wayne State University. Analysis was performed with 20,000 events per sample using the ModFit LT v. 2 for Macintosh data acquisition software package (Verity Software House, Inc.; distributed by Becton Dickinson Immunocytometry System BDIS). Propidium iodide was detected by the FL-2 photomultiplier tube. Fractions of apoptotic cells were quantified by analysis of the sub-G_1 (subdiploid) peak with ModFit cell cycle analysis. The percent distribution of cells in the various stages of the cell cycle (G_o/G_1, S, G_2/M) was also calculated. Cell aggregates were discarded in the flow cytometry analysis by post-fixation aggregate discrimination.

2.10. Data analysis

Data for enzyme and transport assays and ATP and GSH measurements were normalized to the content of cellular protein. All measurements were made on at least three separate cell cultures. Results are expressed as means ± SEM. Significant differences between means were first assessed by a one-way or two-way analysis of variance. When significant *F* values were obtained with the analysis of variance, Fisher's protected least-significance *t*-test was performed to determine which means were significantly different from one another, with two-tail probabilities < 0.05 considered significant.

3. Results

3.1. Cellular energetics

Activities of several enzymes that are indicative of the status of cellular energetics were measured in the NRK-52E cells (Table 1). Where the data are available from earlier studies in either freshly isolated or primary cultures of PT cells from F344 or SD rats, values for the enzyme activities are given to help evaluate the function of the NRK-52E cells. Enzyme activities in the NRK-52E cells and in the various freshly isolated and primary cultured PT cell preparations were assayed under identical conditions, thus allowing comparisons to be made. $(Na^+ + K^+)$-stimulated ATPase activity in NRK-52E cells was only slightly lower than that in freshly isolated PT cells from SD rats but was nearly 50% lower than that in primary cultures of PT cells from SD rats. MDH activity, which is typically very high, was relatively high in NRK-52E cells. In contrast, SDH activity was only 37% of that in freshly isolated PT cells from SD rats. Similarly, GDH activity in NRK-52E cells was 38% lower than that in freshly isolated PT cells from F344 rats but was higher than that in primary cultures of PT cells from both strains of rats. LDH activity, which is indicative of anaerobic energy metabolism, was markedly higher in NRK-52E cells than in freshly isolated or primary cultures of PT cells from both strains of rats. These data suggest that energy metabolism in NRK-52E cells has a modest component of aerobic metabolism but also a significant component of anaerobic metabolism. AP activity, which is a measure of PT cell BBM content, was less than 10% of that in freshly isolated PT cells from both strains and was approximately 25% of that in primary cultures of PT cells from F344 rats. This is consistent with a minimal content of BBMs in this renal PT cell line.

Table 1
Activities of enzymes involved in cellular energetics in NRK-52E cells

Enzyme	Activity (mU/mg protein)				
	NRK-52E[a]	Fresh F344[b]	Fresh SD[b]	Primary F344[b]	Primary SD[b]
$(Na^+ + K^+)$-stimulated ATPase	139 ± 5	–	160, 170 [22,23]	–	260 [24]
Malic dehydrogenase (MDH)	219 ± 6	–	–	–	–
Succinate dehydrogenase (SDH)	22.9 ± 2.3	–	62 [22,23]	–	–
Glutamate dehydrogenase (GDH)	38.6 ± 10.6	62 [21]	–	6 [25]	25 [24]
Lactate dehydrogenase (LDH)	243 ± 3	58, 140 [21]	125, 140, 150 [22,23,26,27]	25 [25]	80 [24]
Alkaline phosphatase (AP)	2.63 ± 0.68	27 [20]	44 [22,23]	10, 13 [25]	–

Enzyme activities were measured by spectrophotometric assays as described in "Materials and methods." Results from the present study using NRK-52E cells are means ± SEM of measurements from three separate cell cultures. Results from the present study are compared to those obtained previously under identical assay conditions in freshly isolated and confluent primary cultures of renal PT cells from Fischer 344 (F344) and Sprague–Dawley (SD) rats. The references from which these previous results were obtained are cited in square brackets. The dashed lines indicate instances in which values were not determined.

[a] Data from the present study.

[b] Data from previously published work.

As the relatively low activities of SDH and GDH and the high activity of LDH suggested that mitochondrial function is diminished in the NRK-52E cells relative to freshly isolated or primary cultures of PT cells, we further investigated mitochondrial function in this cell line. Succinate-stimulated oxygen consumption rates, which are typically 30–40 nmol O_2 consumed/min per mg protein at 37° in freshly isolated PT cells [20], were <10 nmol O_2 consumed/min per mg protein in NRK-52E cells. As these low enzyme and respiratory activities suggest that the NRK-52E cells have a low content of mitochondria relative to freshly isolated or primary cultures of PT cells, we further explored the content of mitochondria in these cells by staining with MitoTracker® Orange (Fig. 1), which accumulates selectively in mitochondria. The cells were examined with a confocal microscope, and the results provide qualitative evidence that the NRK-52E cells have a lower density of mitochondria than native renal PT cells.

The relatively high activity of the $(Na^+ + K^+)$-stimulated ATPase suggests that despite the low rate of succinate-stimulated respiration, NRK-52E cells possess an adequate ATP supply. To characterize the ATP pool, the response of NRK-52E cells to a mitochondrial toxicant was assessed by measurements of ATP content after incubations with either 1 mM IAA + 1 mM KCN (IAA/KCN; used as a positive control) or 10–500 μM DCVC for up to 24 hr (Fig. 2A). Values for ATP contents are shown only for incubations through 4 hr because values at later times exhibited no further changes from the 4-hr values. Cellular content of ATP in control cells at time-zero was 13.6 ± 0.3 nmol/mg protein, which is similar to our previously reported values in freshly isolated PT cells [20,28]. DCVC is a well-characterized nephrotoxicant that has as a very early effect in renal PT cells, inhibition of mitochondrial function and ATP depletion [29,30]. IAA/KCN produced a 51% decrease in cellular content of ATP within 15 min and a maximum amount of ATP depletion of 75%. DCVC also produced a rapid, concentration-dependent decrease in cellular content of ATP. Incubation of cells with 10 μM DCVC for 0.5 hr caused a 38% decrease in ATP content. Maximal amounts of ATP depletion with 4-hr incubations with 10, 50, 100, 200, or 500 μM DCVC ranged from 41 to 59%, increasing in a concentration-dependent manner.

To show that DCVC-induced ATP depletion in NRK-52E cells is dependent upon processes that are known to be involved in freshly isolated PT cells, the effect of the organic anion transport substrate PAH or the cysteine conjugate β-lyase inhibitor AOAA on the extent of DCVC-induced ATP depletion was tested (Fig. 2B). Simultaneous incubation of NRK-52E cells with 1 mM PAH or preincubation for 15 min with 0.1 mM AOAA significantly prevented the ATP depletion induced by 0.2 mM DCVC. This shows that DCVC-induced mitochondrial toxicity in NRK-52E cells, as exemplified by ATP depletion, is dependent upon transport of DCVC into the cell via the organic anion carrier and bioactivation by the cysteine conjugate β-lyase.

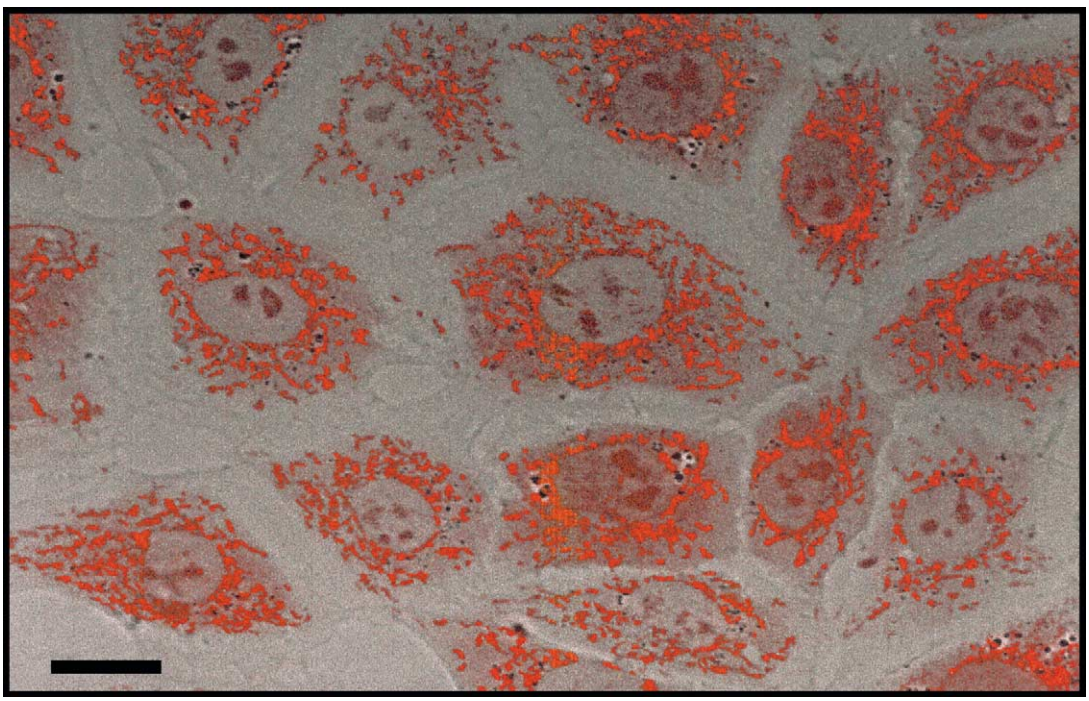

Fig. 1. Fluorescent staining of mitochondria in NRK-52E cells. NRK-52E cells were grown to confluence on collagen-coated glass slides in 35-mm tissue culture dishes. Mitochondria were localized by using a mitochondrial fluorescent marker (MitoTracker® Orange CMTRos). The dye is orange/red with excitation and emission wavelengths of 552 and 576 nm, respectively. Cells were viewed with a Zeiss Triple-Laser Confocal Scanning Microscope. Bar = 5 μm.

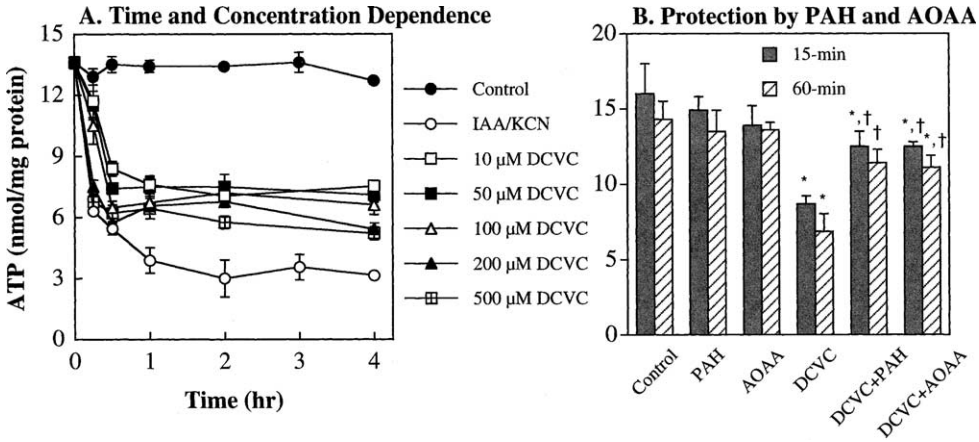

Fig. 2. Chemically induced ATP depletion in NRK-52E cells. NRK-52E cells were grown to confluence on collagen-coated, polystyrene T-25 flasks. The flasks were then incubated for up to 24 hr with either medium (=Control), 1 mM IAA + 1 mM KCN (IAA/KCN), or the indicated concentrations of DCVC. Cellular contents of ATP were measured in perchloric acid extracts of cells by reversed-phase HPLC. (A) Time and concentration dependence of ATP depletion. Results are shown only for incubations up to 4 hr as little or no additional changes were observed in cellular contents of ATP at later time points. Values at the following time points were significantly different ($P < 0.05$) from those of the corresponding control: IAA/KCN—all time points; 10 μM DCVC—all time points except 0.25 hr; 50, 100, 200, and 500 μM DCVC—all time points. (B) Role of organic anion transport and bioactivation by the cysteine conjugate β-lyase on DCVC-induced ATP depletion. Cells were incubated with medium (=0 mM DCVC) or 0.2 mM DCVC for 15 or 60 min. Some of these cells were incubated simultaneously with 1 mM PAH and some were preincubated with 0.1 mM AOAA prior to incubation with DCVC. Results are means ± SEM of measurements from three separate cell cultures. Key: (∗) significantly different ($P < 0.05$) from the corresponding control (=0 mM); and (†) significantly different ($P < 0.05$) from the corresponding sample incubated with DCVC alone.

As a final assessment of the energetics status of NRK-52E cells, we measured the uptake of 1 mM AMG across BBM and BLM in cells grown on filter inserts, which maintains epithelial polarity (Fig. 3). Although the initial rates of AMG uptake across the two membranes were the same, the equilibrium uptake value for transport or cellular accumulation across the BLM was nearly 60% higher than those for transport across the BBM. Hence, the NRK-52E cells have a high capacity to transport glucose, which corresponds with their high rate of anaerobic metabolism.

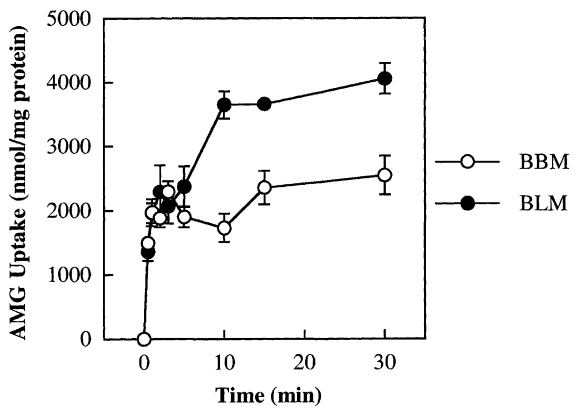

Fig. 3. Uptake of AMG across the BBM and BLM of NRK-52E cells. NRK-52E cells were grown to confluence on Millicell filter inserts in 35-mm tissue culture dishes and were incubated for the indicated times with 1 mM 3-*O*-[^{14}C]AMG. Cells were exposed to AMG from either the BBM side (upper compartment) or the BLM side (lower compartment), and total cellular accumulation was quantified at each time point by scintillation counting. Results are the means ± SEM of measurements from three separate cell culture preparations.

3.2. GSH metabolism and transport

To assess the status of GSH in the NRK-52E cells, we first measured activities of several GSH-dependent or GSH-related enzymes and compared these to activities measured previously in freshly isolated or primary cultures of PT cells from F344 and SD rats (Table 2). As with the measurements of activities of cellular energetics enzymes, measurements of activities of GSH-related enzymes in the NRK-52E, freshly isolated PT, and primary cultures of PT cells were all conducted under identical conditions, thus allowing for direct comparisons to be made. As expected from the data on AP activity (cf. Table 1), the activity of GGT was also very low in the NRK-52E cells. GGT activity in the cell line was only 0.6 to 3.1% of that previously measured in freshly isolated PT cells and was 1.9 to 3.7% of that previously measured in primary cultures of PT cells. In contrast to this marked difference, activities of the other GSH-dependent or GSH-related enzymes were comparable to or only modestly lower than those in freshly isolated or primary cultures of PT cells.

An additional, important aspect of the handling of GSH by renal PT cells is plasma membrane transport [1,2,17,33]. NRK-52E cells were grown on filter inserts and were exposed to 5 mM GSH from either the BLM or BBM side, and the cellular accumulation of GSH was determined (Fig. 4). The initial rate and maximal cellular content of GSH were significantly greater when cells were exposed to GSH on the BLM side as compared to cells exposed to GSH on the BBM side. Moreover, the initial rate of GSH uptake across the BLM was approximately twice that of GSH uptake across the BBM (105 ± 21 vs

Table 2
Activities of GSH-dependent enzymes NRK-52E cells

Enzyme	Activity (mU/mg protein)				
	NRK-52E[a]	Fresh F344[b]	Fresh SD[b]	Primary F344[b]	Primary SD[b]
γ-Glutamyltransferase (GGT)	2.03 ± 0.92	65, 100, 110, 212, 276, 335 [17,20,21,25,31,32]	70, 159 [22,23]	55, 60 [31,32]	105 [24]
Glutathione *S*-transferase (GST)	32.8 ± 3.3	9, 10, 12, 14 [21,31,32]	–	8 [32]	9 [24]
γ-Glutamylcysteine synthetase (GCS)	81.1 ± 12.0	130, 150 [17,32]	70 [23]	75 [32]	70 [24]
Glutathione peroxidase (GPX)	29.0 ± 5.2	42, 52, 63, 92 [21,31,32]	26, 28 [22,23]	45 [32]	60 [24]
Glutathione disulfide reductase (GRD)	24.5 ± 4.8	15, 28, 40, 45 [21,31,32]	17, 27 [22,23]	20 [32]	–

Enzyme activities were measured by spectrophotometric assays as described in "Materials and methods." Results from the present study using NRK-52E cells are means ± SEM of measurements from three separate cell cultures. Results from the present study are compared to those obtained previously under identical assay conditions in freshly isolated and confluent primary cultures of renal PT cells from Fischer 344 (F344) and Sprague–Dawley (SD) rats. The references from which these previous results were obtained are cited in square brackets. The dashed lines indicate instances in which values were not determined.

[a] Data from the present study.

[b] Data from previously published work.

51.3 ± 8.5 nmol/min per mg protein), and maximal or equilibrium cellular accumulation was similarly about 2-fold higher in cells exposed to GSH from the BLM side compared to the BBM side (146 ± 19 vs 81.1 ± 13.5 nmol/mg protein).

Besides transport and GSH-dependent detoxification reactions such as GPX and GST, metabolism of GSH in renal PT cells also involves degradation and oxidation [1,17]. NRK-52E cells were incubated with 0, 1, 2, or 5 mM GSH for up to 60 min, and intracellular contents of GSH, glutamate, cysteine, and GSSG were measured. After 60 min of incubation, a progressive, concentration-dependent increase was observed in GSH content (Table 3). Cells incubated with media containing no added GSH exhibited a 44% loss in their GSH content over 60 min.

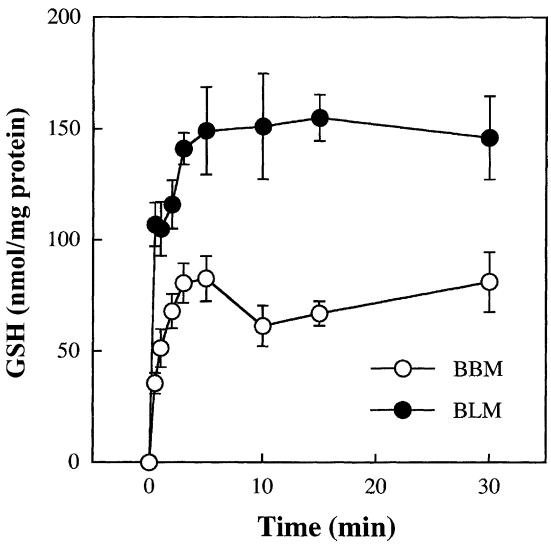

Fig. 4. Uptake of GSH across the BBM and BLM of NRK-52E cells. NRK-52E cells were grown to confluence on Millicell filter inserts in 35-mm tissue culture dishes and were incubated for the indicated times with 5 mM L-[^{3}H-*glycyl*]GSH. Cells were exposed to GSH from either the BBM side (upper compartment) or the BLM side (lower compartment), and total cellular accumulation was quantified at each time point by scintillation counting. Results are the means ± SEM of measurements from four separate cell culture preparations.

No significant changes were observed in the cellular content of glutamate with increasing concentrations of extracellular GSH, suggesting that either no degradation occurred during the 60-min incubation or that any glutamate that was formed was further metabolized and did not accumulate. In the absence of added GSH, no detectable cysteine was measured in the cells after 60 min. A modest increase was observed in cellular contents of cysteine with increasing GSH concentration, suggesting that either a small degree of degradation of GSH did occur over the 60-min incubation, although the maximal increase was only about 3% of that of GSH content, or that the exogenous GSH prevented the loss of cysteine from the cells. GSSG content also increased with increasing exogenous GSH concentration, but again the maximal increase was only about 7% of that of GSH, suggesting that little oxidation occurred.

A final aspect of renal cellular GSH status that was investigated is the subcellular distribution of transported GSH. Transport of GSH across the mitochondrial inner membrane from the cytoplasm is the primary, if not the sole source of this critical reductant and nucleophile for the mitochondrial matrix [34–36]. Distribution of transported GSH into the mitochondria was assessed by incubation of NRK-52E cells with 5 mM GSH, digitonin-fractionation, and analysis of GSH content in cytosolic and mitochondrial fractions (Fig. 5). Cytosolic GSH content increased rapidly with time, reaching a maximal level at 10 min of 107 ± 4 nmol/mg protein. In contrast, mitochondrial GSH content increased relatively slowly, reaching a maximal level of 9.37 ± 2.95 nmol/mg protein at 5 min, which accounts for only 10% of the total cellular GSH content. This suggests that endogenous transport rates for GSH from cytoplasm into mitochondria in NRK-52E cells may be relatively slow.

3.3. Cytotoxicity

As part of our assessment of mitochondrial function in NRK-52E cells, we characterized the response of the cellular ATP pool to a mitochondrial toxicant, DCVC,

Table 3
Uptake and metabolism of GSH in NRK-52E cells

Parameter	Concentration (nmol/mg protein)			
	0 mM GSH	1 mM GSH	2 mM GSH	5 mM GSH
GSH				
0 min	4.80 ± 0.22			
60 min	2.70 ± 0.24*	6.30 ± 0.22*,**	13.6 ± 1.3*,**	32.4 ± 1.4*,**
Glutamate				
0 min	8.90 ± 0.46			
60 min	9.90 ± 0.23	9.40 ± 0.41	9.00 ± 0.42	8.00 ± 0.38
Cysteine				
0 min	0.80 ± 0.07			
60 min	<0.02*	0.70 ± 0.04	1.00 ± 0.04*,**	1.73 ± 0.11*,**
GSSG				
0 min	0.013 ± 0.001			
60 min	<0.01*	0.60 ± 0.05*,**	0.80 ± 0.04*,**	1.10 ± 0.07*,**

Confluent NRK-52E cells were incubated with either medium (=0 mM) or medium containing 1, 2, or 5 mM GSH for up to 60 min. Data are shown for the 60-min incubations. GSH and related thiols, disulfides, and glutamate were measured in perchloric acid extracts of total cell mixtures (=extracellular + intracellular) that were derivatized with IAA and 1-fluoro-2,4-dinitrobenzene by ion-exchange HPLC. Results are means ± SEM of measurements from three separate culture.

* Significantly different ($P < 0.05$) from 0-min, 0-mM GSH control.

** Significantly different ($P < 0.05$) from 60-min, 0-mM GSH sample.

showing that it produced rapid and significant, although incomplete, depletion of the cellular ATP pool (cf. Fig. 2). ATP depletion is also an indication of DCVC-induced cytotoxicity. To explore and characterize DCVC-induced cytotoxicity further, cellular morphology and the occurrence of apoptosis in NRK-52E cells incubated with DCVC or STS, an agent known to produce apoptosis, were determined.

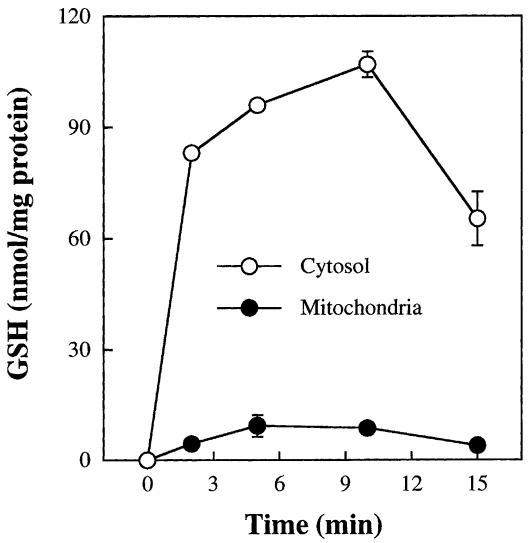

Fig. 5. Subcellular distribution of transported GSH in NRK-52E cells. NRK-52E cells were grown to confluence on collagen-coated T-25 flasks and incubated with 5 mM GSH for the indicated time periods. Cells were then detached from culture flasks by brief treatment with trypsin/EDTA and centrifuged through digitonin to separate cytoplasmic and mitochondrial compartments. GSH content in each compartment was determined by ion-exchange HPLC after derivatization with IAA and 1-fluoro-2,4-dinitrobenzene. Results are the means ± SEM of measurements from four separate cell cultures.

NRK-52E cells that were incubated for 48 hr in culture medium (=Control) were confluent and exhibited normal epithelial morphology, i.e. they contained large centrally located nuclei and were rounded in shape with close intercellular connections (Fig. 6A). In contrast, cultures incubated for 48 hr with 1 μM STS exhibited elongated cells, areas on the culture dish that were denuded of cells, condensed nuclei, and apoptotic bodies (Fig. 6B). Cultures incubated for 48 hr with 10 μM DCVC exhibited many cells that appeared normal, but also several condensed nuclei and a few apoptotic bodies (Fig. 6C). Destruction of cellular morphology progressed with increasing concentrations of DCVC: cultures incubated for 48 hr with 50 μM DCVC exhibited elongated and irregularly shaped cells, areas on the culture dish that were denuded of cells, many condensed nuclei, apoptotic bodies, and intracellular vesicles (Fig. 6D). Cultures incubated for 48 hr with 100 μM DCVC exhibited little apparent normal cellular structure with condensed bodies and numerous jagged projections (Fig. 6E). Finally, cultures incubated for 48 hr with 1 mM DCVC exhibited no recognizable cellular structures (Fig. 6F).

Apoptosis in NRK-52E cells induced by STS (Fig. 7) and DCVC (Fig. 8) was quantitated by flow cytometry and FACS analysis. Cultures incubated for various times up to 48 hr with 1 μM STS exhibited increasing amounts of apoptotic cells, the proportion of which rose to approximately 40% by 24 and 48 hr (Fig. 7). This response demonstrates the appropriate responsiveness of the NRK-52E cells to a "classical" apoptotic-inducing agent.

Cultures were incubated with 0, 10, 50, 100, or 500 μM DCVC for up to 48 hr, and induction of apoptosis and distribution of cells among the phases of the cell cycle were determined by flow cytometry and FACS analysis (Fig. 8).

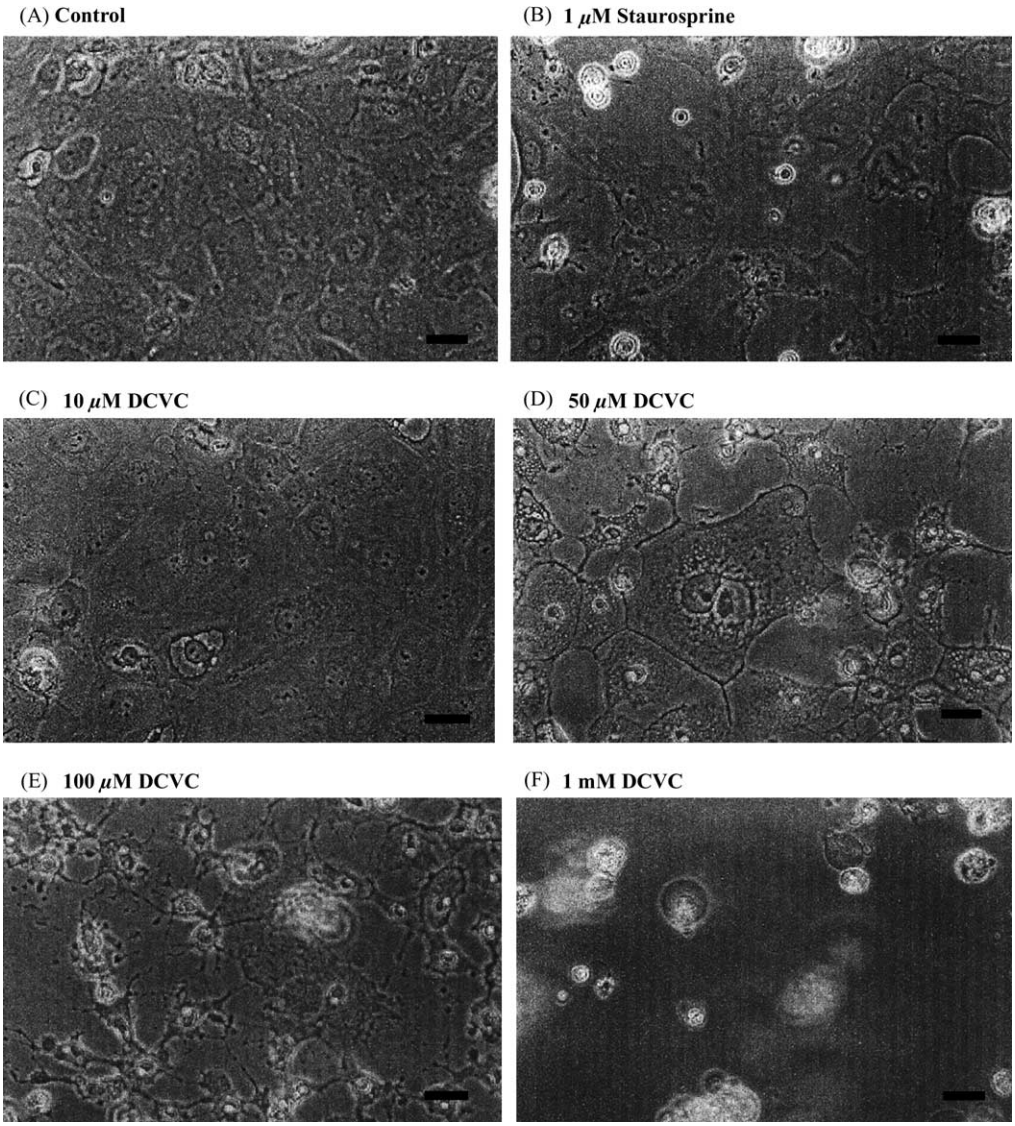

Fig. 6. Photomicrographs of NRK-52E cells incubated with STS or DCVC for 48 hr. Confluent NRK-52E cells were incubated in 35-mm culture dishes for 48 hr with various concentrations of DCVC in cell culture medium. STS (1 μM) was used as a positive control for apoptosis. At the end of the incubation period, photomicrographs were taken at 100× magnification on a Zeiss Confocal Laser Microscope. Bar = 5 μM.

The results show that changes in the distribution of NRK-52E cells among the different phases of the cell cycle and the induction of apoptosis are complex, time- and inducing agent concentration-dependent processes. Although the majority of cells are in the G_0/G_1 phase of the cell cycle, which is due to the near-confluence of the initial cultures, significant changes occurred in the proportion of cells in the other phases of the cell cycle and in those cells undergoing apoptosis. Specifically, a statistically significant increase occurred in the proportion of cells in the S phase and in G_2/M as early as 4 hr with as low a concentration of DCVC as 10 μM, suggesting an increase in cell proliferation. Although increases in S phase cells were also observed at higher concentrations of DCVC and at later incubation times, those in G_2/M were not maintained. The DCVC-induced increases in apoptosis were also observed as early as 4 hr and at as low a concentration of DCVC as 10 μM. The fraction of cells undergoing apoptosis increased with concentration up to 100 μM DCVC at all time points and was lower at 500 μM DCVC, presumably because under conditions of a high concentration of DCVC and prolonged incubation time, ATP depletion was too great and cells underwent necrosis.

4. Discussion

NRK-52E cells are an established cell line derived from normal rat kidney PT cells. The present experiments were undertaken to define basic mitochondrial function and cellular GSH status. Analysis of selected enzyme activities and processes in the NRK-52E cells that are indicative of mitochondrial function indicated that energetics is largely glycolytic. This conclusion is based on the low activities of

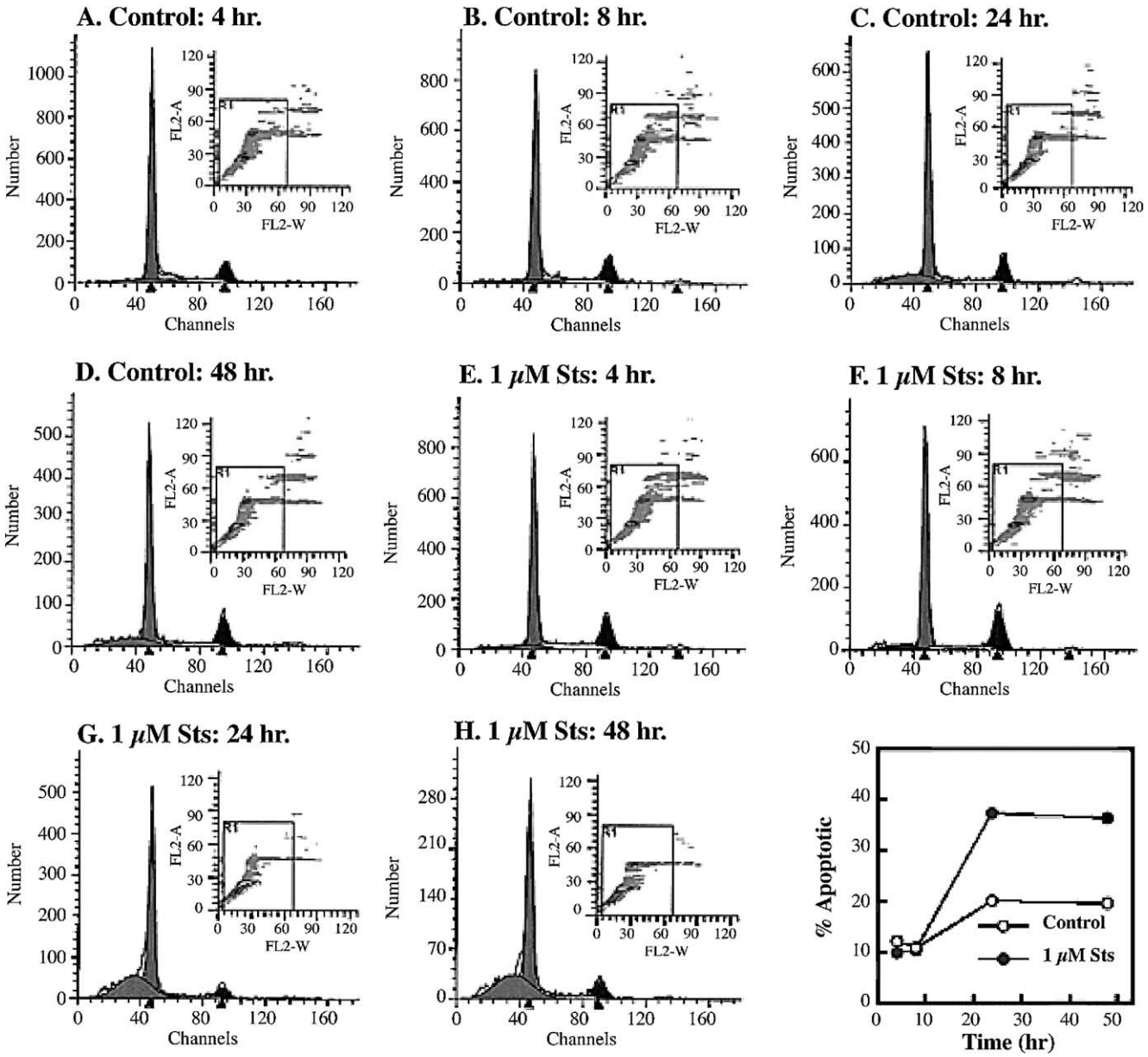

Fig. 7. Flow cytometric analysis of propidium iodide-stained NRK-52E cells treated for up to 48 hr with STS. Confluent NRK-52E cells grown on 35-mm culture dishes were treated for up to 48 hr with either PBS (=Control) or 1 μM STS. Cells were then harvested by trypsin/EDTA treatment, washed in sterile PBS, and fixed overnight in ethanol. Next, cells were stained with propidium iodide and analyzed by flow cytometry with a Becton Dickinson FACS*Calibur* flow cytometer. Panels A–H represent DNA histograms, with cell number (*y*-axis) plotted against DNA content or channel number (*x*-axis). Peaks from left to right represent apoptotic cells, cells in G_0/G_1, cells in S, and cells in G_2/M. The majority of cells (60-80%) are in G_0/G_1 phase with generally less than 10% of cells in S phase. *Insets:* Scatter profiles showing distribution of cells according to propidium iodide fluorescence intensity; *y*-axis = forward scatter; *x-axis* = side scatter. Cells outside the box are those that were excluded from the analysis due to aggregation. Also shown in the lower right-hand corner is a plot of percent apoptotic cells vs time for control cells and cells treated with 1 μM STS.

enzymes such as SDH and GDH, high activities of LDH and AMG transport, and low activity of substrate-stimulated oxygen consumption relative to freshly isolated or primary cultures of rat renal PT cells. In spite of this, the NRK-52E cells exhibited levels of ATP comparable to those of freshly isolated rat renal PT cells and comparable or only modestly lower activity of $(Na^+ + K^+)$-stimulated ATPase, which is one of the primary ATP-consuming reactions in renal PT cells. Microscopic analysis of mitochondrial density, using confocal microscopy and the MitoTracker® Orange fluorescent dye, confirmed that the NRK-52E cells have a much lower density of mitochondria than the *in vivo* proximal tubule, which is not an unexpected finding for an immortalized, epithelial cell line.

Because mitochondrial and nuclear cell division are asynchronous, it is critical to specify the growth state of the cells used in these studies. All measurements of mitochondrial enzymes and confocal microscopy in NRK-52E cells were performed on cells that had just reached confluence. As mitochondrial division may con-

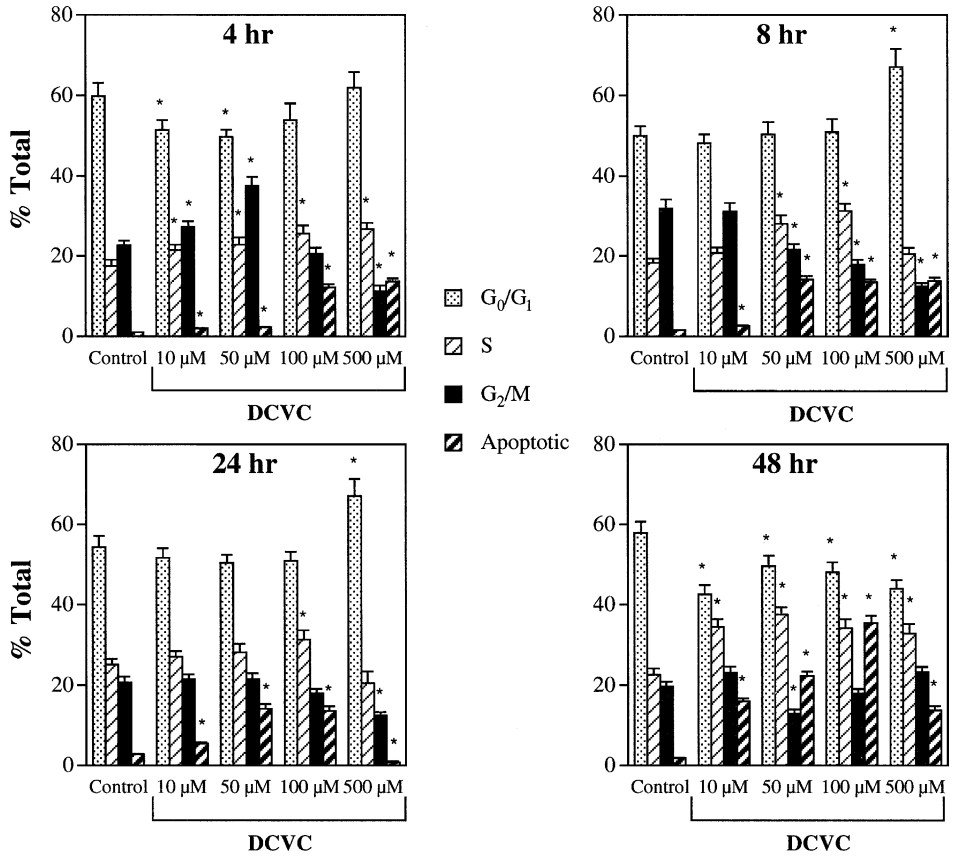

Fig. 8. Time and concentration dependence of changes in cell cycle distribution and apoptosis induced by DCVC treatment of NRK-52E cells. Confluent NRK-52E cells grown on 35-mm culture dishes were treated for 4, 8, 24, or 48 hr with either PBS (=Control) or the indicated concentration of DCVC. At indicated times, samples were processed for FACS analysis as described in the legend to Fig. 7. Results are the means ± SEM of measurements from three separate cell cultures. Key: (∗) significantly different ($P < 0.05$) from the corresponding control sample.

tinue if cells are allowed to grow past confluence, it is possible that mitochondrial enzyme activities and the density of mitochondria as indicated by confocal microscopy may be higher in post-confluent cells than in confluent cells. Such post-confluent cells, however, would not be an appropriate cellular model. An additional consideration is that freshly isolated renal PT cells represent non-dividing cells, whereas primary cultures of PT cells and NRK-52E cells that have just reached confluence represent cells that have divided recently and in which mitochondria may still be undergoing replication. As noted above, comparisons of enzyme activities between the cell line and the primary cultures (cf. Tables 1 and 2) were performed with cells that just reached confluence and assays were performed under identical conditions. Hence, direct comparisons between the primary cultures and the cell line can be made. Although the freshly isolated PT cells may differ in their status of mitochondrial division capacity from the cell culture models, these cells are an important biological model that has been used in numerous studies of metabolism, transport, and acute cytotoxicity. In comparing mitochondrial function, one should, therefore, keep in mind the potential differences in mitochondrial replication capacity among these three cellular models.

To assess the responsiveness of the cellular ATP pool to mitochondrial toxicants, NRK-52E cells were incubated with either IAA/KCN or DCVC. In both cases, significantly less maximal ATP depletion was observed than in similarly treated, freshly isolated renal PT cells [28,30]. Whereas freshly isolated renal PT cells from rats exhibited >95% depletion of cellular ATP after incubation with IAA/KCN [28], a maximal depletion of only 75% was observed in the NRK-52E cells. With DCVC as the toxicant, maximal ATP depletion of 59% with 500 μM DCVC was observed in NRK-52E cells, whereas >80% depletion of cellular ATP was achieved in freshly isolated renal PT cells [30]. Thus, it would appear that a significant portion of the cellular ATP pool in NRK-52E cells is protected from toxicant-induced depletion. This has important implications for the mechanism of chemically induced cell death, because of the requirement for ATP and protein synthesis for apoptosis to occur. As will be discussed below, apoptosis appears to be a prominent mechanism of DCVC-induced cell death in NRK-52E cells.

Partial protection of DCVC-induced ATP depletion by simultaneous incubation with PAH or pretreatment of cells with AOAA confirmed that this cytotoxic response of NRK-52E cells to DCVC exposure was at least partially

due to transport of DCVC into the cell by one of the organic anion carriers and bioactivation by the cysteine conjugate β-lyase, as has been demonstrated in freshly isolated rat renal PT cells [2,5,29,30].

With the exception of GGT activity, the other GSH-dependent or GSH-related enzyme activities exhibited similar levels in NRK-52E cells as are found in freshly isolated or primary cultures of rat renal PT cells. The NRK-52E cells, therefore, have an adequate capacity to use endogenous GSH for defense against reactive electrophiles or oxidants. As is common with renal PT cell lines, such as LLC-PK_1 cells, activities of BBM enzymes such as GGT and AP are very low as compared with the normal, *in vivo* state. This was confirmed by the lack of increases in cellular content of glutamate in NRK-52E cells incubated with up to 5 mM GSH over a 60-min time period. Measurements of cellular accumulation of GSH in NRK-52E cells exposed to 5 mM GSH at either the BBM or BLM surface showed that these cells have a relatively high capacity to transport GSH, and suggest that like freshly isolated PT cells [33,37], the NRK-52E cells have the ability to use exogenous, as well as endogenous, GSH for defense against reactive electrophiles or oxidants.

A major difference in the regulation of cellular GSH status between NRK-52E cells and freshly isolated or primary cultures of renal PT cells concerns mitochondrial GSH. Renal PT cells *in vivo* contain about 30% of their total cellular GSH content within the mitochondria [21,38]. NRK-52E cells incubated with 5 mM GSH, however, contained a maximal proportion of total cellular GSH within the mitochondria of only 10%. Because the renal mitochondrial pool of GSH is determined primarily, if not completely, by transport across the inner membrane from the cytoplasm [34–36], this suggests that either mitochondria in NRK-52E cells have a limited capacity to transport GSH or that there are a relatively low number of mitochondria in these cells. Indeed, measurements of uptake of both GSH and malonate (a characteristic substrate for the dicarboxylate carrier that also transports GSH [34–36]) show that transport rates are relatively low compared to those in renal PT cell mitochondria *in vivo* [39]. These findings are consistent with the conclusion that confluent NRK-52E cells have a low density of mitochondria and low endogenous transport activity for GSH across the mitochondrial inner membrane relative to freshly isolated or primary cultures of PT cells. These characteristics afford us important opportunities to manipulate mitochondrial GSH status.

Besides examination of ATP depletion, the cytotoxicity of DCVC was also assessed by morphology and by quantifying the proportion of cells undergoing apoptosis. NRK-52E cells treated for 48 hr with as low a DCVC concentration as 10 μM exhibited morphological changes consistent with apoptosis (cf. Fig. 6). In contrast, incubation of NRK-52E cells for 48 hr with 50 μM DCVC produced marked cell death with evidence of both apoptosis and necrosis. Incubation with 100 μM DCVC for 48 hr resulted in cultures that exhibited little recognizable cellular structure. Thus, NRK-52E cells are highly sensitive to DCVC. Analysis of cell cycle distribution and the occurrence of subdiploid cells, which are those that are undergoing apoptosis, by flow cytometry and FACS, showed a time- and concentration-dependent increase in the proportion of subdiploid cells. As noted above, the limited extent of ATP depletion induced by DCVC is consistent with an ability to undergo apoptosis. Whereas the proportion of apoptotic cells generally increased with increasing DCVC concentrations up to 100 μM, there was much less apoptosis at 500 μM DCVC. This is consistent with a higher degree of necrosis occurring at higher doses of toxicant. Examination of the time course of DCVC-induced apoptosis in NRK-52E cells showed that cultures incubated for 48 hr actually exhibited a higher proportion of apoptotic cells than cultures incubated for shorter time periods. Cultures also exhibited small, but statistically significant increases in the proportion of cells in the S phase of the cell cycle, which suggests that DCVC can enhance cell proliferation.

An important issue for validation of NRK-52E cells regarding DCVC-induced cytotoxicity is how time and dose dependence and potency compare with responses observed in freshly isolated or primary cultures of rat renal PT cells. Necrosis, as typically measured by LDH release from cells, could not be measured in the NRK-52E cells because of the presence of serum in the culture medium, as this interfered with the assay. Judging by ATP depletion, DCVC would appear to be somewhat less potent in the NRK-52E cells than in freshly isolated or primary cultures of rat renal PT cells, as discussed above. However, some of the results from the present study can be compared with those obtained with primary cultures of rat and human renal PT cells and with another established, renal PT cell line, viz. LLC-PK_1 cells, which are derived from porcine PT cells.

In a study on the cytotoxicity of trichloroethylene and DCVC in primary cultures of rat renal PT cells [32], we showed that DCVC produced acute cellular necrosis, as assessed by increases in LDH release, at concentrations of 0.1 mM and above at incubation times of 2 hr and longer. In longer-term incubations (24 and 72 hr), DCVC concentrations of at least 0.5 mM were required to increase LDH release significantly at either time point, and concentrations of at least 2 mM at incubation times of 72 hr were required to decrease total cellular protein content. One result that we obtained that can be directly compared with those from the present study is an experiment to measure expression of vimentin, which is only found in dedifferentiated PT cells in a cell population that is undergoing repair. We observed that primary cultures of rat renal PT cells that were incubated for 72 hr with 10 μM DCVC showed expression of vimentin. This corresponds with our demonstration of statistically significant increases in

apoptosis and S phase cells in NRK-52E cell cultures treated with 10 μM DCVC.

In contrast to our previous results in primary cultures of rat renal PT cells [32], which suggested that DCVC exhibits a similar potency in the primary cultures and in the NRK-52E cells, two studies by van de Water and colleagues [40,41], using primary cultures of rat renal PT cells and examining DCVC-induced apoptosis, suggest that the primary cultures are significantly less sensitive to DCVC than the NRK-52E cells. Whereas we observed significant increases in numbers of subdiploid cells by FACS and flow cytometry at DCVC concentrations as low as 10 and 50 μM, van de Water and colleagues demonstrated caspase activation and changes in cytoskeletal proteins with DCVC concentrations in the range of 0.1 to 0.25 mM. One must be careful in comparing results in the two systems, however, because of differences in culture conditions that may alter cellular susceptibility. It should be noted, however, that while our previous study in primary cultures of rat renal PT cells used a serum-free, hormonally defined culture medium [32]and the present study in NRK-52E cells used a serum-containing culture medium, the studies by van de Water *et al.* [40,41] used a serum-containing culture medium. Similarly, a study by Chen *et al.* [42] on DCVC-induced apoptosis and mitochondrial dysfunction in LLC-PK_1 cells showed pro-apoptotic effects of DCVC, including DNA fragmentation, caspase activation, and cytochrome *c* release, at concentrations of 0.5 or 1 mM, whereas 0.1 mM DCVC was without effect. As the LLC-PK_1 cells are cultured in a serum-containing medium, their culture conditions may be considered to be similar to those of the NRK-52E cells. Hence, NRK-52E cells are approximately one order of magnitude more sensitive to DCVC-induced apoptosis than are the LLC-PK_1 cells.

We recently completed a study in which time and concentration dependence of DCVC-induced necrosis, apoptosis, and enhanced cell proliferation in primary cultures of human renal PT cells were analyzed in detail [43]. The primary cultures of human renal PT cells, like our primary cultures of rat renal PT cells, were cultured in serum-free, hormonally defined medium, and appear to be more sensitive than the NRK-52E cells to DCVC-induced apoptosis. This conclusion is based on significant apoptosis occurring in the human renal PT cells with 10 μM DCVC as early as 2 hr and maximal apoptosis occurring with 50 μM DCVC in 4–8 hr.

In summary, the results of the present study show that NRK-52E cells exhibit many properties, regarding their cellular energetics and GSH status, that make them a useful model for studies on mitochondrial GSH transport and renal cellular injury. As with most immortalized epithelial cell lines, energetics is largely glycolytic, although mitochondria are present with reduced function relative to the *in vivo* proximal tubule. The NRK-52E cells are sensitive to a mitochondrial toxicant.

Acknowledgments

This work was supported by a National Institute of Diabetes and Digestive and Kidney Diseases grant (R01-DK40725) to L.H.L. Core facilities funded by the National Institute of Environmental Health Sciences Center for Molecular Toxicology with Human Applications (Grant P30-ES06639) at Wayne State University were used for some of these studies.

References

[1] Lash LH. Glutathione and other antioxidant defense mechanisms. In: Goldstein RS, editor. Comprehensive series in toxicology, vol. 7. Oxford: Elsevier; 1997. p. 403–28.
[2] Lash LH, Jones DP, Anders MW. Glutathione homeostasis and glutathione *S*-conjugate toxicity in kidney. Rev Biochem Toxicol 1988;9:29–67.
[3] Woods JS, Kavanagh TJ, Corral J, Reese AW, Diaz D, Ellis ME. The role of glutathione in chronic adaptation to oxidative stress: studies in a normal rat kidney epithelial (NRK52E) cell model of sustained upregulation of glutathione biosynthesis. Toxicol Appl Pharmacol 1999;160:207–16.
[4] Miller C, Kennington L, Cooney R, Kohjimoto Y, Cao LC, Honeyman T, Pullman J, Jonassen J, Scheid C. Oxalate toxicity in renal epithelial cells: characteristics of apoptosis and necrosis. Toxicol Appl Pharmacol 2000;162:132–41.
[5] Elfarra AA, Jakobson I, Anders MW. Mechanism of *S*-(1,2-dichlorovinyl)glutathione induced nephrotoxicity. Biochem Pharmacol 1986;35:283–8.
[6] Bessey OA, Lowry OH, Brock ML. A method for the rapid determination of alkaline phosphatase with five cubic milliliters of serum. J Biol Chem 1946;164:321–9.
[7] Schoner W, von Ilberg C, Kramer R, Seubert W. On the mechanism of Na^+- and K^+-stimulated hydrolysis of adenosine triphosphate. 1. Purification and properties of a Na^+- and K^+-activated ATPase from ox brain. Eur J Biochem 1967;1:334–43.
[8] Fleischer S, Fleischer B. Removal and binding of polar lipids in mitochondria and other membrane systems. Methods Enzymol 1967;10:406–33.
[9] Schmidt E, Schmidt FW. Glutamate dehydrogenase. In: Bergmeyer HU, editor. Methods of enzymatic analysis, vol. III, 3rd ed. Weinheim: Verlag Chemie; 1983. p. 216–27.
[10] Kornberg A. Lactic dehydrogenase of muscle. Methods Enzymol 1955;1:441–54.
[11] Ochoa S. Malic dehydrogenase from pig heart. Methods Enzymol 1955;1:735–9.
[12] Seelig GF, Meister A. γ-Glutamylcysteine synthetase from erythrocytes. Anal Biochem 1984;141:510–4.
[13] Lawrence RA, Burk RF. Glutathione peroxidase activity in selenium-deficient rat liver. Biochem Biophys Res Commun 1976;71:952–8.
[14] Eklöw L, Moldéus P, Orrenius S. Oxidation of glutathione during hydroperoxide metabolism: a study using isolated hepatocytes and the glutathione reductase inhibitor 1,3-bis(2-chloroethyl)-1-nitrosourea. Eur J Biochem 1984;138:459–63.
[15] Orlowski M, Meister A. γ-Glutamyl-*p*-nitroanilide: a new convenient substrate for determination and study of L- and D-γ-glutamyltranspeptidase activities. Biochim Biophys Acta 1963;73:679–81.
[16] Habig WH, Pabst MJ, Jakoby WB. Glutathione *S*-transferases: the first enzymatic step in mercapturic acid formation. J Biol Chem 1974;249:7130–9.
[17] Visarius TM, Putt DA, Schare JM, Pegouske DM, Lash LH. Pathways of glutathione metabolism and transport in isolated proximal tubular cells from rat kidney. Biochem Pharmacol 1996;52:259–72.

[18] Fariss MW, Reed DJ. High-performance liquid chromatography of thiols and disulfides: dinitrophenyl derivatives. Methods Enzymol 1987;143:101–9.
[19] Jones DP. Determination of pyridine nucleotides in cell extracts by high-performance liquid chromatography. J Chromatogr 1981;225: 446–9.
[20] Lash LH, Tokarz JJ. Isolation of two distinct populations of cells from rat kidney cortex and their use in the study of chemical-induced toxicity. Anal Biochem 1989;182:271–9.
[21] Lash LH, Visarius TM, Sall JM, Qian W, Tokarz JJ. Cellular and subcellular heterogeneity of glutathione metabolism and transport in rat kidney cells. Toxicology 1998;130:1–15.
[22] Lash LH, Zalups RK. Activities of enzymes involved in renal cellular glutathione metabolism after uninephrectomy in the rat. Arch Biochem Biophys 1994;309:129–38.
[23] Lash LH, Zalups RK. Alterations in renal cellular glutathione metabolism after *in vivo* administration of a subtoxic dose of mercuric chloride. J Biochem Toxicol 1996;11:1–9.
[24] Lash LH, Putt DA, Zalups RK. Biochemical and functional characteristics of cultured renal epithelial cells from uninephrectomized rats: factors influencing nephrotoxicity. J Pharmacol Exp Ther 2001;296:243–51.
[25] Lash LH, Tokarz JJ, Pegouske DM. Susceptibility of primary cultures of proximal tubular and distal tubular cells from rat kidney to chemically induced toxicity. Toxicology 1995;103:85–103.
[26] Lash LH, Zalups RK. Mercuric chloride-induced cytotoxicity and compensatory hypertrophy in rat kidney proximal tubular cells. J Pharmacol Exp Ther 1992;261:819–29.
[27] Lash LH, Putt DA, Zalups RK. Influence of exogenous thiols on mercury-induced cellular injury in isolated renal proximal tubular and distal tubular cells from normal and uninephrectomized rats. J Pharmacol Exp Ther 1999;291:492–502.
[28] Lash LH, Tokarz JJ, Chen Z, Pedrosi BM, Woods EB. ATP depletion by iodoacetate and cyanide in renal distal tubular cells. J Pharmacol Exp Ther 1996;276:194–205.
[29] Lash LH, Anders MW. Mechanism of *S*-(1,2-dichlorovinyl)-L-cysteine- and *S*-(1,2-dichlorovinyl)-L-homocysteine-induced renal mitochondrial toxicity. Mol Pharmacol 1987;32:549–56.
[30] Lash LH, Anders MW. Cytotoxicity of *S*-(1,2-dichlorovinyl)glutathione and *S*-(1,2-dichlorovinyl)-L-cysteine in isolated rat kidney cells. J Biol Chem 1986;261:13076–81.
[31] Lash LH, Tokarz JJ. Oxidative stress in isolated rat renal proximal and distal tubular cells. Am J Physiol 1990;259:F338–47.
[32] Cummings BS, Zangar RC, Novak RF, Lash LH. Cytotoxicity of trichloroethylene and *S*-(1,2-dichlorovinyl)-L-cysteine in primary cultures of rat renal proximal tubular and distal tubular cells. Toxicology 2000;150:83–98.
[33] Lash LH, Putt DA. Renal cellular transport of exogenous glutathione: heterogeneity at physiological and pharmacological concentrations. Biochem Pharmacol 1999;58:897–907.
[34] McKernan TB, Woods EB, Lash LH. Uptake of glutathione by renal cortical mitochondria. Arch Biochem Biophys 1991;288:653–63.
[35] Chen Z, Lash LH. Evidence for mitochondrial uptake of glutathione by dicarboxylate and 2-oxoglutarate carriers. J Pharmacol Exp Ther 1998;285:608–18.
[36] Chen Z, Putt DA, Lash LH. Enrichment and functional reconstitution of glutathione transport activity from rabbit kidney mitochondria: further evidence for the role of the dicarboxylate and 2-oxoglutarate carriers in mitochondrial glutathione transport. Arch Biochem Biophys 2000;373:193–202.
[37] Hagen TM, Aw TY, Jones DP. Glutathione uptake and protection against oxidative injury in isolated kidney cells. Kidney Int 1988;34: 74–81.
[38] Schnellmann RG, Gilchrist SM, Mandel LJ. Intracellular distribution and depletion of glutathione in rabbit renal proximal tubules. Kidney Int 1988;34:229–33.
[39] Lash LH, Putt DA, Matherly LH. Protection of normal rat kidney-52E cells, a rat renal proximal tubular cell line, from chemical-induced apoptosis by overexpression of a mitochondrial glutathione transporter. J Pharmacol Exp Ther, in press.
[40] van de Water B, Kruidering M, Nagelkerke JF. F-Actin disorganization in apoptotic cell death of cultured rat renal proximal tubular cells. Am J Physiol 1996;270:F593–603.
[41] van de Water B, Nagelkerke JF, Stevens JL. Dephosphorylation of focal adhesion kinase (FAK) and loss of focal contacts precede caspase-mediated cleavage of FAK during apoptosis in renal epithelial cells. J Biol Chem 1999;274:13328–37.
[42] Chen Y, Cai J, Anders MW, Stevens JL, Jones DP. Role of mitochondrial dysfunction and *S*-(1.2-dichlorovinyl)-L-cysteine-induced apoptosis. Toxicol Appl Pharmacol 2001;170:172–80.
[43] Lash LH, Hueni SE, Putt DA. Apoptosis, necrosis and cell proliferation induced by *S*-(1,2-dichlorovinyl)-L-cysteine in primary cultures of human proximal tubular cells. Toxicol Appl Pharmacol 2001;177: 1–16.